

Dynamic Structural Response Analysis of Flexible Rolled-Up Solar Array Subjected to Deformation-Dependent Thermal Loading

Masahiko Murozono
Kyushu University, Fukuoka 819-0395, Japan

Key Words : Thermoelasticity, Solar array, Dynamic response, Radiant heating, Self-excited vibration

Abstract

Theoretical studies in the thermally induced dynamic structural response of an asymmetric rolled-up solar array and its stability are presented. Structural response analysis of the solar array subjected to deformation-dependent thermal loading was conducted considering with the thermoelastic coupling effect. The governing equations and the time dependent boundary conditions are formulated assuming that the solar array is heated by the unidirectional radiation and that net heat input depends on the angle of incidence of radiation with respect to the array axis. Quasi-static responses of the solar array induced by external radiant heating were calculated, and it was shown that the difference of several percent arose in the steady-state value of the tip deflection between the case of coupled analysis and the case of uncoupled analysis. Dynamic responses of the solar array induced by sudden radiation heating for a typical night-day orbital transition were determined and the stability of the system was discussed. Variations of the dynamic response are examined. The response becomes either a self-excited vibration or a damped vibration with the system parameters such as radiation incident angle. Unstable boundary curves, which divide the parameter plane into regions of stability and instability according to the direction of radiation and system damping ratio, are also presented.

1. Introduction

The problem of structural vibration due to thermal effects was introduced by Boley¹⁾, who has taken structural inertia effects into account but no notice of influences of deformations upon temperature distributions. A number of review articles^{2),3)} about thermally induced vibrations in aerospace applications have appeared.

A series of research has been done starting with the failure of the Hubble Space Telescope solar array with a kink about midway along its length. Thornton and Kim⁴⁾ describe an analysis of the thermally induced bending vibrations of a symmetric flexible rolled-up solar array model. Uncoupled and coupled thermal-structural dynamics responses were studied using an analytical model restricted to symmetric bending deformations of the solar array. Chung and Thornton⁵⁾ focused on a torsional analysis of a symmetric FRUSA model. A torsional buckling analysis was conducted using an analytical model restricted to antisymmetric torsional deformations of the solar array. However, an HST solar array is not exactly symmetric about its centerline; its solar blanket is shifted slightly toward the outer BiSTEM. Even though the solar array was heated by uniform radiation, coupled bending-torsional deformations occur because of the asymmetry. Murozono and Thornton⁶⁾ presented an theoretical analyses of the buckling characteristics and the quasistatic thermal-structural responses of an asymmetric

FRUSA model. One of the results of the analyses considering the geometric asymmetry suggested that thermally induced quasistatic torsional deformation may have caused the failure of the HST solar array BiSTEM. Dynamic thermal-structural responses of the same asymmetric solar array model were also studied by the authors. Although the analyses showed quasistatic and dynamic thermally induced structural responses, the analyses did not consider the coupling of temperature fields and deformations.

Thermally induced bending vibrations of thin-walled boom subjected to external radiant heating have been investigated^{7),8)} considering the deformation-dependent thermal loading and the thermal-structural coupling effects. A theoretical analysis was carried out, in which the boom was modeled as an uniform thin-walled circular section cantilever beam or the same beam with a concentrated tip mass at the free end, and experimental verifications of the analysis executed under laboratory conditions both in air and in a vacuum chamber. The experiment showed that unstable bending vibrations can occur when the incident radiation is large.

This paper describes a coupled thermal-structural analysis of an asymmetric FRUSA model to determine a better understanding of the response of the solar array subjected to deformation-dependent thermal loading. Basic equations of the heat conduction and the quasistatic and the dynamic

structural responses of the solar array subjected to sudden radiant heating for a typical night-day orbital transition are formulated. Numerical calculations are presented for the HST solar array to show the difference quantitatively between coupled and uncoupled responses. Stability boundaries and the dynamic structural responses of the solar array both in stable and in unstable regions are also presented.

2. Solar Array Model

The Hubble Space Telescope solar array in-orbit configuration consists of two identical wing-like structures. Each wing has two flexible solar blankets that are deployed from a drum mounted on a shaft cantilevered from the spacecraft. Each solar blanket is unfurled by a rotating actuator mechanism that pushes the two BiSTEM booms from the drum. The deployed ends of the BiSTEMs are connected to a spreader bar to which the solar blanket is attached. A BiSTEM is made from thin stainless-steel tapes formed into circular open cross sections. In their stored configuration, each tape is flattened and stored on a spool within the drum mechanism. During deployment, the stored elastic energy in the flattened tape assists the unfurling mechanisms as each STEM extends and curls back to its original shape forming a BiSTEM with seams diametrically opposed. The spreader bar houses a mechanism that compensates for a slight difference in the BiSTEMs lengths. The storage drum houses a torque mechanism that maintains blanket tension. Thus, during orbital operations, the blanket tension on the spreader bar exerts a compressive force on each BiSTEM.

The mathematical model and coordinate system used in the subsequent analyses are shown in Fig.1. The solar array length and the half spreader bar length are denoted by L and b , respectively. The model assumes that 1) the solar blanket is an inextensible membrane whose thermal expansions and contractions are neglected, 2) the solar blanket is subjected to uniform tension in the x direction, and the membrane tensile force F_x per unit width is constant, 3) the inner and outer BiSTEM booms are identical cantilevered beams subjected to different axial compressive force P_1 and P_2 , respectively, 4) torsional rotations are sufficiently small so that BiSTEM's bending displacements occur only in the x - z plane, 5) thermal expansions of the BiSTEMs are neglected, and 6) the spreader bar is a rigid member of length $2b$ and supports the membrane tensile force over a length b_1+b_2 . For the determination of the temperature distributions, the BiSTEM booms are assumed to be one-piece thin-walled circular section beams.

When the solar blanket is subjected to uniform tensile force F_x per unit width, the inner and the

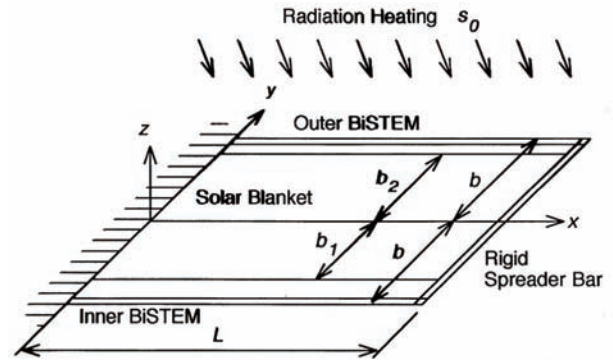


Fig. 1 Solar array analytical model.

outer BiSTEM booms are subjected to axial compressive forces P_1 and P_2 , respectively. The compressive axial forces are determined by considering force equilibrium of the spreader bar in the x direction and moment equilibrium about the z axis. The results may be represented as

$$P_i = P_{fi}P, \quad i=1,2 \quad (1)$$

where

$$P_{f1} = 1 - \frac{b_2 - b_1}{2b}, \quad P_{f2} = 1 + \frac{b_2 - b_1}{2b} \quad (2)$$

and the subscripts 1 and 2 denote the inner and the outer BiSTEMs, respectively. The average axial compressive force P of the BiSTEMs is defined by

$$P = (1/2)F_x(b_1 + b_2) \quad (3)$$

3. Formulations

3.1 Thermal Analysis

Here, a brief description of the perturbation temperature of the BiSTEM boom is given. Detailed discussions of the thermal analysis are found in Refs. 7 and 11. Coupled thermal-structural analyses will be presented based on the assumption that the absorbed heat flux is affected by the boom's deformation. A deformed boom with the incident heat flux s_0 is shown in Fig. 2. The solar array is subjected to an incident solar heat flux s_0 that varies as a step function with time from the direction inclined to the vertical by the angle θ . In writing the energy conservation equation, the heat flux absorbed by the boom is the component normal to the surface. Because of bending, a normal to the beam surface has rotated through a small angle equal to the beam slope. Then, the incident normal heat flux to the

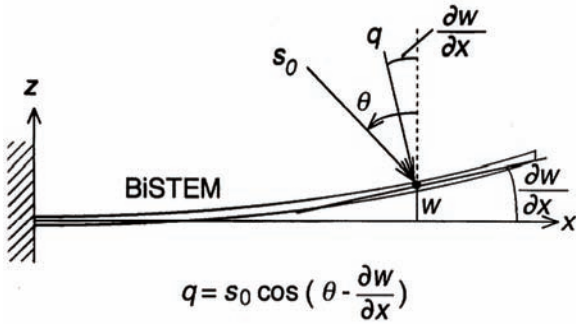


Fig.2 Heat flux for coupled thermal-structural analysis

surface can be expressed by

$$q = s_0 \cos\left(\theta - \frac{\partial w_i}{\partial x}\right) \quad (4)$$

where w_1 and w_2 are deflections of the inner and the outer BiSTEMs, respectively. After the thin walled circular boom is idealized by some heat transfer assumptions⁷⁾, conservation of energy including circumferential conduction and radiation from the external surface yields

$$\frac{\partial T_i}{\partial t} - \frac{k}{\rho c R^2} \frac{\partial^2 T_i}{\partial \phi^2} + \frac{\varepsilon_s \sigma}{\rho c h} T_i^4 = \frac{\alpha_s q}{\rho c h} \delta \cos \phi \quad (5)$$

where k , ρ , and c are the thermal conductivity, the mass density, and the specific heat of the BiSTEM, respectively, R and h are the radius and the wall thickness of the BiSTEM cross section, ε_s and α_s are the thermal emissivity and the thermal absorptivity of the boom surface, and σ is the Stefan-Boltzmann constant. And where ϕ is the angular coordinate of the BiSTEM cross section and parameter δ indicates that only front half of the boom is heated.

$$\begin{cases} \delta = 1 & , \quad -\pi/2 \leq \phi \leq \pi/2 \\ \delta = 0 & , \quad \pi/2 < \phi < 3\pi/2 \end{cases} \quad (6)$$

The temperature distribution is represented as the sum of an average temperature $\bar{T}_i(x, t)$ and a perturbation temperature $T_{mi}(x, t) \cos \phi$, that is

$$T_i(x, \phi, t) = \bar{T}_i(x, t) + T_{mi}(x, t) \cos \phi \quad (7)$$

where the amplitude of the perturbation temperature is assumed small compared with the average temperature so that $T_{mi}/\bar{T}_i \ll 1$. In addition, the heat flux distribution is presented as a truncated

Fourier series with higher order terms neglected. With these assumptions, substituting Eq.(7) into Eq.(5) yields an ordinary differential equation for the average temperature and an equation for the perturbation temperature.,

$$\frac{\partial \bar{T}_i}{\partial t} + \frac{\varepsilon_s \sigma}{\rho c h} \bar{T}_i^4 = \frac{1}{\pi} \frac{\alpha_s s_0}{\rho c h} \cos\left(\theta - \frac{\partial w_i}{\partial x}\right), \quad i=1, 2 \quad (8)$$

$$\begin{aligned} \frac{\partial T_{mi}}{\partial t} + \left(\frac{k}{\rho c R^2} + \frac{4\varepsilon_s \sigma}{\rho c h} \bar{T}_i^3\right) T_{mi} \\ = \frac{1}{2} \frac{\alpha_s s_0}{\rho c h} \cos\left(\theta - \frac{\partial w_i}{\partial x}\right), \quad i=1, 2 \end{aligned} \quad (9)$$

At steady state, the incident heat flux approaches a constant value which is approximated by neglecting the BiSTEM's slope. The steady-state average temperature is given from Eq.(8) as

$$T_{ss} = \left(\frac{1}{\pi} \frac{\alpha_s s_0}{\varepsilon_s \sigma} \cos \theta\right)^{1/4} \quad (10)$$

Assuming that the term \bar{T}_i^3 on the left-hand side of Eq.(9) may be approximated as T_{ss}^3 produce a linear differential equation for T_{mi} . The thermal bending moment M_{Ti} is defined as an integration over a cross section by

$$M_{Ti} = \int_A E \alpha \Delta T(x, \phi, t) z dA \quad (11)$$

where E is the Young's modulus, α is the coefficient of thermal expansion, and ΔT denotes a BiSTEM's cross-sectional temperature gradient. Linear equation is solved to yield T_{mi} and the thermal bending moment can then be obtained as

$$M_{Ti}(x, t) = \frac{EI \alpha T^*}{R \tau} \int_0^t \exp\left(-\frac{t-p}{\tau}\right) \cos\left(\theta - \frac{\partial w_i}{\partial x}\right) dp \quad (12)$$

where

$$T^* = \frac{1}{2} \frac{\alpha_s s_0}{\rho c h} \tau \quad (13)$$

$$\begin{aligned} \frac{1}{\tau} &= \frac{k}{\rho c R^2} + \frac{4\varepsilon_s \sigma}{\rho c h} T_{ss}^3 \\ &= \frac{k}{\rho c R^2} + \frac{4\varepsilon_s \sigma}{\rho c h} \left(\frac{1}{\pi} \frac{\alpha_s s_0}{\varepsilon_s \sigma} \cos \theta\right)^{3/4} \end{aligned} \quad (14)$$

The temperature T^* denotes the steady-state value of the perturbation temperature, and the parameter τ is a characteristic thermal response time. The temperature distribution at a BiSTEM boom cross section is represented as the sum of the average temperature and the perturbation temperature. Among these terms, the perturbation temperature that varies over the cross-section induces a thermal bending moment that causes the BiSTEM boom to bend.

3.2 Structural Analysis

We now consider the coupled thermal-structural response of the solar array when both BiSTEM booms are subjected to the same uniform radiation heating. The structural analysis is performed using equations of motion for the boom bending, boom torsion, and the solar blanket. The equations are solved under the boundary conditions at the support and the interface conditions at the spreader bar. First, considering effects of the compressive axial forces, the partial differential equations and the boundary conditions for BiSTEM bending are

$$L_{1i}[w_i] = EI \frac{\partial^4 w_i}{\partial x^4} + P_i \frac{\partial^2 w_i}{\partial x^2} + \frac{\partial^2 M_{Ti}}{\partial x^2} + \rho A \frac{\partial^2 w_i}{\partial t^2} = 0, \quad i=1,2 \quad (15)$$

$$w_i(0,t) = 0, \quad \frac{\partial w_i}{\partial x}(0,t) = 0, \quad M_{yi}(L,t) = 0; \quad i=1,2 \quad (16)$$

where $w_i(x,t)$ is the BiSTEM boom deflection, EI is the BiSTEM bending stiffness, ρA is the mass per unit length, and M_{yi} is the bending moment defined by

$$M_{yi} = -EI \frac{\partial^2 w_i}{\partial x^2} - M_{Ti}, \quad i=1,2 \quad (17)$$

and M_{Ti} is given in Eq.(11).

The partial differential equations and the corresponding boundary conditions for the BiSTEM boom torsional deformation including the axial compressive force effects are expressed as follows:

$$L_{2i}[w_i] = EI \frac{\partial^4 \theta_{xi}}{\partial x^4} - (GJ - \frac{P_i I_E}{A}) \frac{\partial^2 \theta_{xi}}{\partial x^2} + I_x \frac{\partial^2 \theta_{xi}}{\partial t^2} = 0, \quad i=1,2 \quad (18)$$

$$\theta_{xi}(0,t) = 0, \quad \frac{\partial \theta_{xi}}{\partial x}(0,t) = 0, \quad \frac{\partial \theta_{xi}}{\partial x}(L,t) = 0; \quad i=1,2 \quad (19)$$

where $\theta_{xi}(x,t)$ is the BiSTEM angle of twist, EI is the BiSTEM warping stiffness, GJ is the torsional stiffness, I_E , A , I_x are the polar moment of inertia, cross-sectional area, and the mass moment of inertia per unit length, respectively. The latter two boundary condition means that the BiSTEM cross section is restrained from warping at both ends.

The solar blanket is modeled as a membrane with constant tension F_x per unit width. The tension F_y perpendicular to F_x is neglected since the membrane has a high aspect ratio and the transverse edges of the membrane are free. The equation of motion and the boundary conditions for vibration of the membrane are expressed as

$$L_3[w_m] = -F_x \frac{\partial^2 w_m}{\partial x^2} + \sigma_m \frac{\partial^2 w_m}{\partial t^2} = 0 \quad (20)$$

$$w_m(0,y,t) = 0, \quad w_m(L,y,t) = w_{sd}(y,t) \quad (21)$$

where $w_m(x,y,t)$ is the solar blanket deflection, σ_m is the solar blanket mass per unit area, and w_{sd} is the spreader bar deflection. Because we assume that the spreader bar is rigid, w_{sd} may be written using the deflection of its center of mass, w_{s0} , and the rotation angle of the spreader bar θ_{s0} . For small rotations the deflection and the rotation of the spreader bar are presented using the tip deflections of the BiSTEMs as

$$w_{sd}(y,t) = w_{s0}(t) + y\theta_{s0}(t) = \frac{1}{2}\{w_1(L,t) + w_2(L,t)\} + \frac{y}{2b}\{w_2(L,t) - w_1(L,t)\} \quad (22)$$

3.3 Approximate Solution

Because the thermal bending moment depends on the BiSTEM boom slope that appears in the integrand of Eq.(12), a modal representation of the solution could not be obtained. Then, an approximate solution based on the method of weighted residuals is developed. The solutions for the BiSTEM boom deflection and rotation and the solar blanket deflection are taken in the form

$$\begin{aligned} w_i(x,t) &= W_i(x)U(t), \quad i=1,2 \\ \theta_{xi}(x,t) &= \Theta_i(x)U(t), \quad i=1,2 \\ w_m(x,y,t) &= W_m(x,y)U(t) \end{aligned} \quad (23)$$

where the approximate functions $W_i(x)$, $\Theta_i(x)$, and $W_m(x,y)$ are assumed to satisfy the geometric boundary conditions. In the following calculations, functions that represent the deformation obtained in the quasistatic thermal-structural response analysis are used as the approximate functions. The method of weighted residuals is based on

$$\int_{\Omega} R(x,t)W(x)dx = 0 \quad (24)$$

where $R(x,t)$ is the residual obtained from substituting an approximate solution into a differential equation, and $W(x)$ is a weighting function. In the present analysis, the approximate functions are used as the weighting functions according to the Galerkin's method. Thus, residual form for the governing equation can be written as

$$\begin{aligned} & \int_0^L L_{11}[w_1]W_1(x)dx + \int_0^L L_{12}[w_2]W_2(x)dx \\ & + \int_0^L L_{21}[\theta_{x1}]\Theta_1(x)dx + \int_0^L L_{22}[\theta_{x2}]\Theta_2(x)dx \quad (25) \\ & + \int_0^L \int_{-b_1}^{b_2} L_3[w_m]W_m(x,y)dydx = 0 \end{aligned}$$

To consider the mass M_s and mass moment of inertia I_s of the spreader bar, both the mass distribution ρA and distribution of the mass moment of inertia I_x are replaced as follows:

$$\begin{aligned} \rho A & \rightarrow \rho A + \frac{1}{2} M_s \delta(x-L) \\ I_x & \rightarrow I_x - I_s \delta(x-L) \end{aligned} \quad (26)$$

where $\delta(x)$ denotes the delta function.

Introducing the approximations for w_i , θ_{xi} , and w_m from Eq.(23) and integrating the special derivatives by parts, an ordinary differential equation for the unknown function $U(t)$ is obtained as

$$\ddot{U} + \omega_0^2 U = \frac{1}{M} F(t) \quad (27)$$

where ω_0 is an approximate value to the first mode natural frequency

$$\omega_0 = \sqrt{K/M} \quad (28)$$

And K , M , and $F(t)$ are the stiffness, mass, and force, respectively, for the equivalent single degree of freedom system and are written as follows:

$$\begin{aligned} K & = EI \int_0^L \{(W_1'')^2 + (W_2'')^2\} dx \\ & - \int_0^L \{P_1(W_1')^2 + P_2(W_2')^2\} dx \\ & + EI \int_0^L \{(\Theta_1'')^2 + (\Theta_2'')^2\} dx \\ & + \int_0^L \{(GJ - \frac{P_1 I_E}{A})(\Theta_1')^2 + (GJ - \frac{P_2 I_E}{A})(\Theta_2')^2\} dx \\ & + F_x \int_0^L \int_{-b_1}^{b_2} (W_m')^2 dydx \end{aligned} \quad (29)$$

$$\begin{aligned} M & = \rho A \int_0^L (W_1^2 + W_2^2) dx \\ & + I_x \int_0^L (\Theta_1^2 + \Theta_2^2) dx + \sigma_m \int_0^L \int_{-b_1}^{b_2} W_m^2 dydx \\ & + M_s \left\{ \frac{1}{2} [(W_1(L) + W_2(L))]^2 \right. \\ & + I_s \left\{ \frac{1}{2b} [W_2(L) - W_1(L)]^2 \right. \\ & + \frac{1}{2} M_s \{ W_1^2(L) + W_2^2(L) \} \\ & \left. \left. - I_s \{ \Theta_1^2(L) + \Theta_2^2(L) \} \right. \right. \end{aligned} \quad (30)$$

$$\begin{aligned} F(t) & = - \int_0^L W_1''(x) M_{T1}(x,t) dx \\ & - \int_0^L W_2''(x) M_{T2}(x,t) dx \end{aligned} \quad (31)$$

Both the stiffness K and the mass M depend on the shapes of the approximate functions and the geometric and physical properties of the solar array, and independent from the thermal properties such as the heat flux s_0 , characteristic thermal response time τ , and the incident angle θ . Approximate functions for the BiSTEM bending and torsion used here are written as follows:

$$\begin{aligned} W_i(x) & = \alpha_i \{ \tan \lambda_i L (1 - \cos \lambda_i x) - (\lambda_i x - \sin \lambda_i x) \} \\ & - \frac{1}{P_{fi}} \frac{1 - \cos \lambda_i x}{\cos \lambda_i L} \end{aligned} \quad (32)$$

$$\Theta_i(x) = \gamma_i \{ \sinh \beta_i L (\sinh \beta_i x - \beta_i x) - (1 - \cosh \beta_i L)(1 - \cosh \beta_i x) \} \quad (33)$$

For the solar blanket deflection, the approximate function is expressed as

$$W_m(x, y) = \frac{x}{L} (W_{s0} + y \Theta_{s0}) \quad (34)$$

where the deflection of the center of mass of the spreader bar W_{s0} is given

$$W_{s0} = \frac{1}{2} \{ \alpha_1 (\tan \lambda_1 L - \lambda_1 L) + \alpha_2 (\tan \lambda_2 L - \lambda_2 L) \} - \frac{1}{2} \left(\frac{1}{P_{f1}} \frac{1 - \cos \lambda_1 L}{\lambda_1 L} + \frac{1}{P_{f2}} \frac{1 - \cos \lambda_2 L}{\lambda_2 L} \right) \quad (35)$$

and

$$\Theta_{s0} = \frac{1}{2b} \{ \alpha_2 (\tan \lambda_2 L - \lambda_2 L) - \alpha_1 (\tan \lambda_1 L - \lambda_1 L) \} - \frac{1}{2b} \left(\frac{1}{P_{f2}} \frac{1 - \cos \lambda_2 L}{\lambda_2 L} - \frac{1}{P_{f1}} \frac{1 - \cos \lambda_1 L}{\lambda_1 L} \right) \quad (36)$$

Detailed discussions of the quasistatic thermal-structural response analysis are found in Ref.6. Parameters λ_i and β_i ($i=1, 2$) are defined in terms of the compressive axial force of the BiSTEM by

$$\lambda_i^2 = \frac{P_i}{EI}, \quad \beta_i^2 = \frac{1}{EI} \left(GJ - \frac{P_i I_E}{A} \right); \quad i=1, 2 \quad (37)$$

The parameter α_i ($i=1, 2$), which determine the magnitude of the BiSTEM bending deflection, is obtained by solving the simultaneous equations given by

$$\begin{bmatrix} C_{11} & C_{12} \\ C_{21} & C_{22} \end{bmatrix} \begin{Bmatrix} \alpha_1 \\ \alpha_2 \end{Bmatrix} = \begin{Bmatrix} g_1 \\ g_2 \end{Bmatrix} \quad (38)$$

where each term of the coefficient matrix C_{ij} ($i, j=1, 2$) is determined by the BiSTEM compressive axial forces and properties of the solar array as

$$C_{11} = \frac{P_1}{L} \tan \lambda_1 L \quad (39a)$$

$$C_{12} = \frac{P_2}{L} \tan \lambda_2 L \quad (39b)$$

$$C_{21} = P_1 b \lambda_1 + P b \frac{\tan \lambda_1 L - \lambda_1 L}{L} \times \left(\frac{b_2^2 - b_1 b_2 + b_1^2}{3b^2} - \frac{b_2 - b_1}{2b} \right) + \frac{\tan \lambda_1 L - \lambda_1 L}{2b} \sum_{i=1}^2 \left(GJ - \frac{P_i I_E}{A} \right) \times \frac{\beta_i \sinh \beta_i L}{\beta_i L \sinh \beta_i L + 2(1 - \cosh \beta_i L)} \quad (39c)$$

$$C_{22} = -P_2 b \lambda_2 - P b \frac{\tan \lambda_2 L - \lambda_2 L}{L} \times \left(\frac{b_2^2 - b_1 b_2 + b_1^2}{3b^2} + \frac{b_2 - b_1}{2b} \right) - \frac{\tan \lambda_2 L - \lambda_2 L}{2b} \sum_{i=1}^2 \left(GJ - \frac{P_i I_E}{A} \right) \times \frac{\beta_i \sinh \beta_i L}{\beta_i L \sinh \beta_i L + 2(1 - \cosh \beta_i L)} \quad (39d)$$

The terms on the right-hand side of the equation are defined as

$$g_1 = \frac{1}{L} \left(\frac{1 - \cos \lambda_1 L}{\cos \lambda_1 L} + \frac{1 - \cos \lambda_2 L}{\cos \lambda_2 L} \right) \quad (40a)$$

$$g_2 = \frac{b}{L} \left\{ \frac{1}{P_{f1}} \frac{1 - \cos \lambda_1 L}{\cos \lambda_1 L} \left(\frac{b_2^2 - b_1 b_2 + b_1^2}{3b^2} - \frac{b_2 - b_1}{2b} \right) - \frac{1}{P_{f2}} \frac{1 - \cos \lambda_2 L}{\cos \lambda_2 L} \left(\frac{b_2^2 - b_1 b_2 + b_1^2}{3b^2} + \frac{b_2 - b_1}{2b} \right) \right\} - \frac{1}{2Pb} \left(\frac{1}{P_{f2}} \frac{1 - \cos \lambda_2 L}{\cos \lambda_2 L} - \frac{1}{P_{f1}} \frac{1 - \cos \lambda_1 L}{\cos \lambda_1 L} \right) \times \sum_{i=1}^2 \left(GJ - \frac{P_i I_E}{A} \right) \frac{\beta_i \sinh \beta_i L}{\beta_i L \sinh \beta_i L + 2(1 - \cosh \beta_i L)} \quad (40b)$$

The magnitude parameter γ_i ($i=1, 2$) for the BiSTEM angle of twist is obtained as

$$\gamma_i = - \frac{\Theta_{s0}}{\beta_i L \sinh \beta_i L + 2(1 - \cosh \beta_i L)}, \quad i=1, 2 \quad (41)$$

The numerator is the BiSTEM tip angle of twist. It is given by Eq.(36).

Because the thermal bending moments appearing in Eq.(31) contain the BiSTEM boom slope $\partial w_i / \partial x$ in the cosine term inside of an integral as shown in Eq.(12), which represents the coupling between the structural and the thermal responses, the equivalent single-degree-of-freedom equation remains difficult to solve analytically. Then, Eq.(31) can be linearized by approximating the cosine term inside of an integral based on the assumption that the BiSTEM boom's slope is small as

$$\cos(\theta - \frac{\partial w_i}{\partial x}) \cong \cos \theta + \frac{\partial w_i}{\partial x} \sin \theta, \quad i = 1, 2 \quad (42)$$

Using the approximation and considering the system damping, the ordinary differential equation of the unknown function $U(t)$ becomes a linear equation as

$$\ddot{U} + 2\zeta\omega_0\dot{U} + \omega_0^2 U = \frac{1}{M} F(t) \quad (43)$$

where ζ is the damping ratio, and

$$\omega_0 = \sqrt{K/M}$$

The force $F(t)$ appearing in the right-hand side of Eq.(43) still contains the unknown function inside of integrals

$$\begin{aligned} F(t) = & -\frac{EI\alpha T^*}{R\tau} \left\{ \int_0^L \int_0^t W_1''(x) \exp(-\frac{t-p}{\tau}) \right. \\ & \times [\cos \theta + W_1'(x)U(p) \sin \theta] dp dx \\ & + \int_0^L \int_0^t W_2''(x) \exp(-\frac{t-p}{\tau}) \\ & \left. \times [\cos \theta + W_2'(x)U(p) \sin \theta] dp dx \right\} \quad (44) \end{aligned}$$

3.4 Quasistatic Responses

To evaluate the effect of thermo-elastic coupling quantitatively, quasistatic responses are obtained by neglecting the effect of inertia term. Equation for the unknown function $U(t)$ has the form as

$$KU = F(t) \quad (45)$$

With the Laplace transform for the convolution integrals and the inverse transform, a solution is obtained as

$$U(t) = -\frac{A \cos \theta}{K + B \sin \theta} (1 - e^{-Ct}) \quad (46)$$

Where K is the stiffness defined in Eq. (29), and parameters A , B , and C are defined as follows

$$A = \frac{EI\alpha T^*}{R} \left(\int_0^L W_1'' dx + \int_0^L W_2'' dx \right) \quad (47)$$

$$B = \frac{EI\alpha T^*}{R} \left(\int_0^L W_1'' W_1' dx + \int_0^L W_2'' W_2' dx \right)$$

$$C = \frac{1}{\tau} \left(1 + \frac{B}{K} \right) \sin \theta \quad (48)$$

Quasistatic structural responses of the solar array are calculated by using Eq.(23) with Eq. (46).

3.5 Dynamic Responses and Stability Criterion

The dynamic responses and the stability of them of the solar array are determined by obtaining the Laplace transform of the differential equation.

$$\begin{aligned} s^2 \bar{U}(s) + 2\zeta\omega_0 s \bar{U}(s) + \omega_0^2 \bar{U}(s) \\ = -\frac{1}{M} \frac{1}{\tau s + 1} \left\{ \frac{A \cos \theta}{s} + B \sin \theta \cdot \bar{U}(s) \right\} \quad (49) \end{aligned}$$

The dynamic response is calculated by inversion of the Laplace transform $\bar{U}(s)$ obtained by solving Eq. (49) to yield $U(t)$. The inverse transform can be practiced analytically by solving the cubic equation and using the inverse transform for convolution integrals. Approximate solutions are given by Eq. (23) with the $U(t)$. The characteristic equation can be written in the dimensionless form as

$$q(\bar{s}) = \bar{s}^3 + (2\zeta + \kappa)\bar{s}^2 + (1 + 2\zeta\kappa)\bar{s} + \kappa(1 + \eta) = 0 \quad (50)$$

where

$$\bar{s} = \frac{s}{\omega_0}, \quad \kappa = \frac{1}{\omega_0 \tau}, \quad \eta = \frac{B}{K} \sin \theta \quad (51)$$

In the last equation, K is the stiffness by Eq. (29) and B is defined in Eq. (47). The parameter κ means the ratio of the characteristic mechanical response time to the characteristic thermal response time and its inverse number $1/\kappa$ is an equivalent to the nondimensional parameter used by Boley¹²⁾ in the analysis of thermally induced bending vibration of beams. The parameter η is in direct proportion to the

intensity of the heat flux s_0 and is also dependent on the direction of the radiation heating θ . From the Routh-Hurwitz stability criterion, following condition is required for a stable response.

$$\eta < \frac{2\zeta(\kappa^2 + 2\zeta\kappa + 1)}{\kappa} \quad (52)$$

Because ζ and κ are positive quantities, right-hand side of the equation is always positive. Thus, the stability criterion shows that negative or zero incident angles of solar radiation heating, $\theta \leq 0$, produce stable responses.

4. Numerical Calculation Results

Numerical calculations presented hereafter use data^{9),10)} for the HST solar arrays as shown in Table 1. The BiSTEM material is stainless steel.

4.1 Quasistatic Thermal Structural Responses

Since it is expected that structural responses

Table 1 Solar array properties of the HST

Solar array length	$L=5.91$ m
Half width	$b=1.428$ m
Solar heat flux	$s_0=1.350 \times 10^3$ W/m ²
Stefan-Boltzmann constant	$\sigma=5.670 \times 10^{-8}$ W/(m ² K ⁴)
Solar blanket	
Width	b_1+b_2 $b_1=1.138$ m $b_2=1.249$ m
Mass per unit area	$\sigma_m=1.589$ kg/m ²
Spreader bar	
Mass	$M_s=1.734$ kg
Mass moment of inertia	$I_s=1.179$ kgm ²
BiSTEM	
Cross-sectional area	$A=1.613 \times 10^{-5}$ m ²
Bending stiffness	$EI=1.711 \times 10^2$ Nm ²
Warping stiffness	$EF=4.991 \times 10^{-1}$ Nm ⁴
Torsional stiffness	$GJ=6.503 \times 10^{-3}$ Nm ²
Polar moment of inertia	$I_E=1.948 \times 10^{-9}$ m ⁴
Mass moment of inertia per unit length	$I_x=1.348 \times 10^{-5}$ kgm ² /m
Density	$\rho=7.010 \times 10^3$ kg/m ³
Wall thickness	$h=2.35 \times 10^{-4}$ m
Radius	$R=1.092 \times 10^{-2}$ m
Specific heat	$c=5.020 \times 10^2$ J/(kgm)
Thermal conductivity	$k=1.661 \times 10^1$ W/(mK)
Coefficient of thermal expansion	$\alpha=1.629 \times 10^{-5}$ 1/K
Thermal absorptivity	$\alpha_s=0.5$
Thermal emissivity	$\epsilon_s=0.13$

significantly vary with P , the average axial compressive force P is assumed to take the design value 14.75 N unless otherwise specified. The quasistatic structural response of the BiSTEM tip deflection was calculated using Eq. (46) to evaluate the effect of thermo-elastic coupling quantitatively. Figure 3 shows time histories of the BiSTEM tip deflections and the distributions of the steady-state deflections when the solar array is heated from a direction within the fixed-end side, $\theta > 0$. Figure 4 shows the responses when the solar array is heated from a direction of the tip-end side, $\theta < 0$. Quasistatic responses calculated based on the uncoupled analysis, that the temperature is independent of the deflection or the slope of the BiSTEM boom, are also shown in these figures. Because the temperature difference between the heated and the unheated sides increases with time, the deflections also increase with time. Figures 3 and 4 show that deflections of the outer and the inner BiSTEMs are different in spite of the uniform heating, due to the coupled bending-torsional deformations because of the geometric asymmetry of the solar array. Figure 3 shows that coupled thermo-elastic responses are slightly smaller than the uncoupled calculation results when the incident angle θ is positive. Contrary to this, Fig. 4

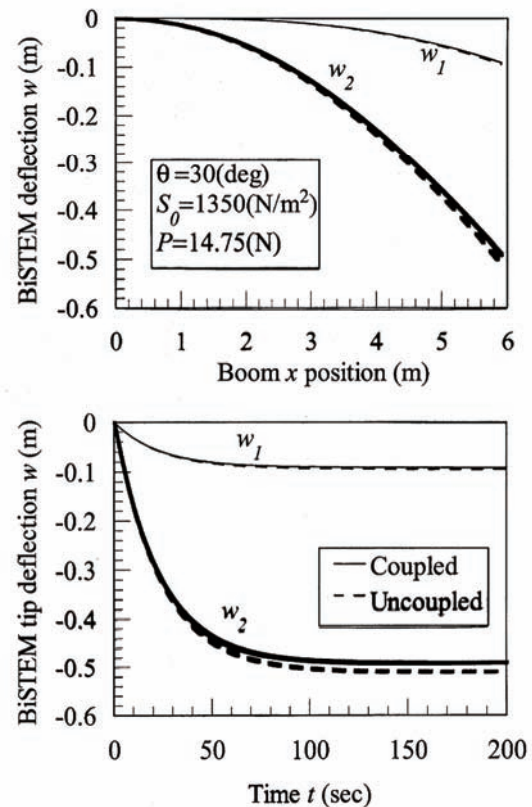


Fig.3 Quasistatic responses of the solar array subjected to uniform radiation heating from the direction $\theta=\pi/6$.

shows that deflections calculated based on the coupled analysis are larger than that of the uncoupled analysis when the angle θ is negative. Variations of the steady-state tip deflections of the BiSTEM obtained by the coupled analysis with the solar incident angle θ are shown in Fig. 5 for several values of the axial force P . Because the deformations are almost pure bending when P is small, the curves are shown for $P > 12$ N. It is clearly shown that the largest value of the tip deflection occurs at the case of $\theta \cong 0$ in which the solar array is heated from the direction normal to the undeflected boom axis.

Next, we examine the variation of the effect of the thermoelastic coupling with the radiation heat incident angle θ . Because time histories are considered to be essentially similar to the results shown in Figs. 3 and 4, we only consider the steady-state deflections of the BiSTEM. The thermoelastic coupling effect on the quasistatic responses is determined quantitatively using the relative difference defined as

$$|\Delta| = \left| \frac{w_{coupled} - w_{uncoupled}}{w_{uncoupled}} \right| \quad (53)$$

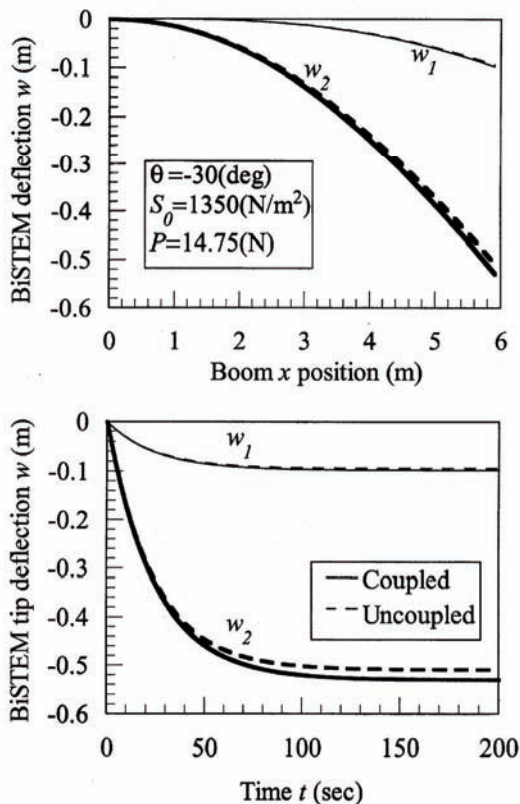


Fig.4 Quasistatic responses of the solar array subjected to uniform radiation heating from the direction $\theta = -\pi/6$.

where $w_{coupled}$ and $w_{uncoupled}$ are the steady-state deflections calculated by the coupled and the uncoupled analyses, respectively. Figure 6 shows variation of $|\Delta|$ with the angle θ . The horizontal axis uses an absolute value of θ . When the heat incident angle θ approaches $\pm\pi/2$, the parameter of the effects of thermoelastic coupling $|\Delta|$ becomes large although the magnitudes of the deflections themselves become small.

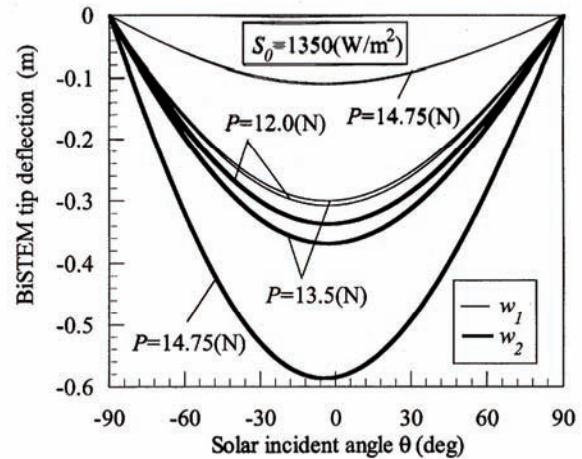


Fig.5 Variations of BiSTEM tip deflections with the solar incident angle θ .

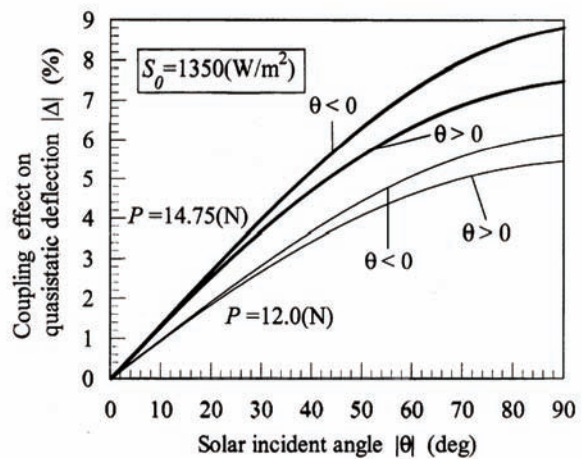


Fig.6 Quantitative effect of the thermoelastic coupling on quasistatic responses of the solar array.

4.2 Stability Boundaries and Dynamic Responses

According to the stability criterion given in Eq. (52), the stability boundary curves which divide the parameter plane into stable and unstable regions are shown in Fig. 7. The vertical axis of the figure is the

angle θ that measures the inclination of the radiant heat flux from the vertical and on the horizontal axis is the system damping ratio ζ . The stability criterion shows that the response is unconditionally stable for $\theta \leq 0$. There exists the lower limit value of the damping ratio ζ that the system is stable, and if the damping ratio is lower than the critical value then the responses will be unstable. Boundary curves for the asymmetric and the symmetric solar array models are drawn in solid line and dotted line, respectively. It is shown that the unstable region is enlarged when the solar blanket moves toward the outer BiSTEM. Although the results are not shown, the stability boundary also depends on the axial compressive force P . Calculation for the asymmetric solar array model shows that the unstable region is enlarged as the axial force P becomes large.

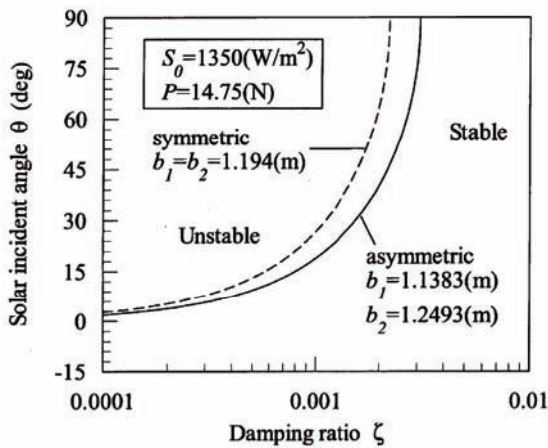


Fig.7 Stability boundaries in the θ - ζ parameter plane

The dynamic responses based on the coupled analyses can be determined from the inverse Laplace transform of $U(s)$ in Eq. (49) and substitution into Eq. (23). The procedure used in calculations of responses are as follows: solve the cubic characteristic equation to obtain three roots for the parameter s , expand $U(s)$ into a partial fraction decomposition, and practice inverse Laplace transform of $U(s)$ by using the convolution integrals. In order to demonstrate the thermoelastic coupled structural responses, deflection time histories for stable, unstable, and neutral cases were calculated. Figure 8 presents time histories of the BiSTEM tip deflections at the stability boundary. The steady-state vibrations with constant amplitude about the quasistatic deflections are shown. Because of bending-torsional coupling, torsional deformation causes the difference between quasistatic deflections of the inner and the outer BiSTEMs. Figure 9 presents time histories of the BiSTEM tip deflections both in stable and in

unstable regions. Stable responses for a solar radiation incident angle $\theta=15$ deg in the upper figure show that the quasistatic deflection of the outer BiSTEM is much larger than that of the inner BiSTEM and vibrations about the quasistatic deflections decay with time. In contrast, unstable responses for an incident angle $\theta=60$ deg show that a self-excited vibration occurs. Because of the large incident angle θ , only a small amount of the radiant heat flux is absorbed by the BiSTEM boom, then the magnitude of the total response becomes relatively small in the case of $\theta=60$ deg.

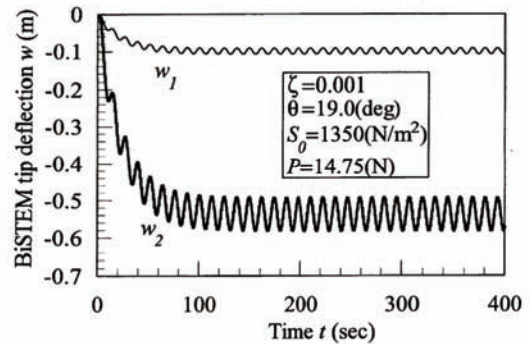


Fig.8 BiSTEM boom deflection time histories at the stability boundary

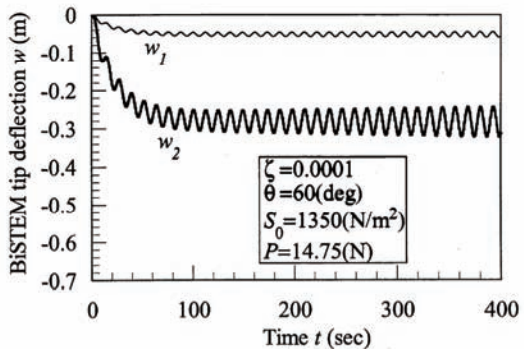
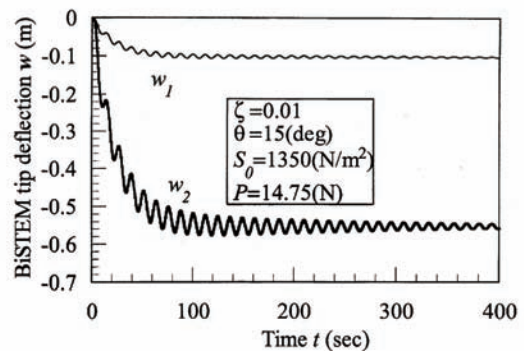


Fig. 9 Stable and unstable time histories of the BiSTEM boom tip deflection from the coupled analysis

The occurrence mechanism of the self-excited vibration or thermal flutter depends on the time-dependent radiation heat flux. The amount of heat flux absorbed by the BiSTEM boom is determined by the angle between the incident radiation heat flux and a normal to the boom surface. In the case of $\theta > 0$, when the boom deflects toward the radiant heat flux, the net incident angle decreases and the absorbed heat flux increases. When the boom deflects in the opposite direction, the net incident angle increases and the absorbed heat flux decreases. If the boom is vibrating, these variations of heat flux produce the time-dependent temperature gradient, and so time-varying thermal bending moment.

5. Conclusions

Theoretical analyses of the coupled thermal-structural responses of an asymmetric flexible rolled-up solar array were presented. The analyses were based on a generalized flexible rolled-up solar array model assuming asymmetric loading conditions because of geometric asymmetry. The coupled thermal-structural analysis includes the effects of structural deformation on external heating and temperature gradients. Numerical calculations were conducted using the data for the solar arrays of the HST.

An approximate solution was obtained by using the method of weighted residuals for the coupled thermal-structural responses of the solar array model. Effects of thermoelastic coupling were estimated quantitatively by calculating the quasistatic responses based on both the coupled and the uncoupled theories. The differences between the calculated results of the coupled and the uncoupled steady-state tip deflections of the BiSTEM booms are 9 % at the most.

Stability criterion and the dynamic coupled thermal-structural responses were also presented. According to the closed form stability criterion, the boundary curves which divide the parameter plane into stability and instability regions were shown. System parameters in determining the stability include the ratio of the structural and thermal response times, radiant heat incident angle, and the system damping. Dynamic structural responses of the solar array subjected to sudden radiation heating such as typical night-day transition in orbit were presented for stable, unstable, and the neutral cases. The time history of tip deflection in the unstable region shows the occurrence of thermal flutter.

References

- 1) Boley, B. A., "Thermally Induced Vibrations of Beams," *Journal of the Aeronautical Sciences*, Vol.3, No.2, 1956, pp.179-181.
- 2) Malla, R. B. and Ghoshal, A., "Thermally Induced Vibrations of Structures in Space," *Aerospace Thermal Structures and Materials for a New Era*, edited by E. A. Thornton, Progress in Astronautics and Aeronautics, Vol.168, 1995, pp.68-95.
- 3) Thornton, E. A., *Thermal Structures for Aerospace Applications*, AIAA, 1996, pp.343-396.
- 4) Thornton, E. A. and Kim, Y. A., "Thermally Induced Bending Vibrations of a Flexible Rolled-Up Solar Array," *Journal of Spacecraft and Rockets*, Vol.30, No.4, 1993, pp.438-448.
- 5) Chung, P. W. and Thornton, E. A., "Torsional Buckling and Vibration of a Flexible Rolled-Up Solar Array," AIAA Paper 95-1355, April 1995.
- 6) Murozono, M. and Thornton, E. A., "Buckling and Quasistatic Thermal-Structural Response of Asymmetric Rolled-Up Solar Array," *Journal of Spacecraft and Rockets*, Vol.35, No.2, 1998, pp.147-155.
- 7) Murozono, M. and Sumi, S., "Thermally Induced Bending Vibrations of Thin-Walled Boom with Closed Section by Radiant Heating," *Memoirs of the Faculty of Engineering, Kyushu University*, Vol.49, No.4, 1989, pp.273-290.
- 8) Murozono, M. and Sumi, S., "Thermal Flutter of Thin-Walled Circular Section Beams Subjected to Radiant Heating," *Proceedings of the IV Conference of Asian-Pacific Congress on Strength Evaluation*, 1991, pp.676-681.
- 9) Reynolds, J., "The Analysis of the Deployed Space Telescope Solar Array," European Space Agency, ESA Doc. TN-SA-B142, British Aerospace, Bristol, England, UK, Jan. 1983.
- 10) "STEM Design Characteristics and Parameters," Astro Aerospace Corp., TR AAC-B-006, Carpinteria, CA, Sept. 1985.
- 11) Rimrott, F. P. J. and Abdel-Sayed, R., "Flexural Thermal Flutter Under Laboratory Conditions," *Transactions of the Canadian Society for Mechanical Engineering*, Vol.4, No.4, 1977, pp.189-196.
- 12) Boley, B. A., "Approximate Analyses of Thermally Induced Vibrations of Beams and Plates," *Transactions of the ASME, Journal of Applied Mechanics*, Vol.39, No.1, 1972, pp.212-216.